Effect of Energetic Secondary Electrons on the Scintillation Process in Alkali Halide Crystals

AXEL MEYER AND R. B. MURRAY
Solid-State Division, Oak Ridge National Laboratory, Oak Ridge, Tennessee*
(Received May 28, 1962)

Experimental results have previously shown that the scintillation efficiency of alkali halide crystals to heavy particles is not a function of dE/dx alone but is instead composed of a series of discrete functions, one for each incident particle. This paper presents an analysis of these experimental results with attention to the effect of energetic secondary electrons (delta rays) produced by the primary particle. In this treatment the total light emitted per unit path length of the incident particle is the sum of two contributions: one from the highly ionized primary column, and one from those delta rays which escape the primary column and produce light with a high efficiency.

INTRODUCTION

THE response of activated alkali iodide scintillators to heavy charged particles exhibits a decreasing scintillation efficiency with increasing specific energy loss of the primary particle. This behavior has been frequently ascribed to "saturation of luminescence centers" in the wake of a highly ionizing particle. This saturation mechanism has been examined theoretically in a proposed model of the scintillation process.[1] In this model scintillation efficiency is defined as dL/dE, differential light output per unit energy loss, and is taken to be a single-valued function of specific energy loss, dE/dx, of the incident particle.

Experiments with the heavy ion accelerator at Yale[2,3] indicate, however, that the scintillation efficiency of NaI(Tl) and CsI(Tl) to heavy particles is not a function of dE/dx alone but is instead composed of a series of discrete functions, one for each incident particle. These results are illustrated in Fig. 1 for the case of NaI(Tl). The ordinate of Fig. 1 has been normalized to unity for protons of 8 to 10 MeV. It is clear that these curves cannot be represented by a single function of dE/dx. The experimental results in Fig. 1 in fact indicate that, for a given dE/dx, the scintillation efficiency depends sensitively on the identity of the incident particle. For example, at a stopping power of 2000 keV-cm^2/mg the scintillation efficiency of O^{16} is about twice that of C^{12}. This behavior is, at first sight, quite surprising as it indicates that the scintillation mechanism distinguishes between two particles of nearly the same mass which have exactly the same dE/dx.

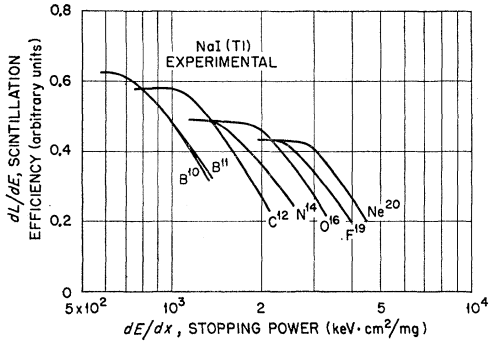

FIG. 1. Experimental scintillation efficiency vs dE/dx for heavy ions B^{10} through Ne^{20} in NaI(Tl), taken from Newman and Steigert, reference 2. The ordinate is normalized such that the scintillation efficiency to protons in the 10-MeV region is 1.0. In the terminology of the present paper the ordinate is $(dL/dE)_t$ and the abscissa is $(dE/dx)_t$.

This paper presents an interpretation of the experimental results of Fig. 1, with particular attention to the role of energetic secondary electrons (delta rays) created by the heavy primary particle.

ANALYSIS OF EXPERIMENTAL RESULTS

The over-all behavior of the scintillation efficiency decreases with increasing dE/dx for all particles from protons to fission fragments, as indicated in the previous review.[1] This general trend is apparent in the data of Fig. 1, where it is seen that the maximum scintillation efficiency of each particle (corresponding to the horizontal portion of each curve) declines with increasing atomic number or increasing dE/dx. This over-all behavior points to a basic light-producing mechanism which is associated with the ionization density in the wake of the primary particle. (This will be referred to later as the primary light source.) The discrete nature of the curves in going from one particle to another represents a kind of "fine structure" on the gross behavior, and indicates that the basic light-producing mechanism is in some way modified by the identity of the primary particle. We are thus led to seek some property of the energy loss process which differs for two particles of exactly the same dE/dx but different atomic number. The most obvious property is the energy distribution of secondary electrons resulting from ionizing collisions of the primary with electrons of the stopping medium. If the delta rays are sufficiently energetic to escape from the immediate wake of the primary particle, they can then enter a

* Oak Ridge National Laboratory is operated by Union Carbide Corporation for the U. S. Atomic Energy Commission.

[1] R. B. Murray and A. Meyer, Phys. Rev. **122**, 815 (1961).

[2] E. Newman and F. E. Steigert, Phys. Rev. **118**, 1575 (1960).

[3] E. Newman, A. M. Smith, and F. E. Steigert, Phys. Rev. **122**, 1520 (1961).

virgin region of the crystal and produce light with their characteristic high efficiency.

The maximum energy of a delta ray resulting from a primary particle of energy E is given by the Rutherford scattering formula as $\epsilon_0^{\max}=4m(E/M)$, neglecting the electron mass m in comparison to the mass M of the primary. (This assumes that the struck electron is initially at rest; this approximation will be made throughout.) Thus, the maximum energy of the delta ray spectrum is proportional to the energy per nucleon E/A of the primary. At the same time, consideration of dE/dx as a function of energy for heavy particles reveals that, for two different particles of the same dE/dx, the particle of greater nuclear charge has a greater value of E/A. (This may be readily seen in Fig. 3 of reference 2 after multiplying the ordinate by A to obtain dE/dx (MeV-cm^2/mg) as a function of E/A. Note that the labels B^{10} and B^{11} are interchanged, and that for these two particles (of the same z) dE/dx is the same function of E/A.) Thus, for two different primary particles having the same dE/dx, the higher-z particle produces a more energetic spectrum of delta rays and is therefore expected to yield a higher scintillation efficiency. This is seen to be the general case in Fig. 1. The foregoing statements may be illustrated qualitatively with the Bethe stopping-power expression, from which dE/dx is found to be proportional to $[z^2/(E/A)]\ln(KE/A)$, where K is a property of the stopping medium. In the energy region of interest here ($E/A>1$ MeV per nucleon) dE/dx is a decreasing function of E/A and the dependence on the logarithmic term is weak compared to the E/A denominator. Thus, for two incident particles of the same dE/dx but having different charge, $z_2>z_1$, it follows that $(E/A)_2>(E/A)_1$. It may also be noted that for two particles of the same z but different mass (e.g., B^{10} and B^{11}) at the same dE/dx, then $(E/A)_2=(E/A)_1$. The delta-ray spectra will be the same, and the scintillation efficiencies should be the same. This is, in fact, found to be the case (see Fig. 1). It should be understood that differences in the delta-ray spectra for two different particles of the same dE/dx arise because of the difference in z, so that the effect discussed in this paper is basically a charge-dependent effect. It is easy to lose sight of this fact since the key parameter is E/A which is associated with the mass of the primary particle.

The analysis to be given below is based on the foregoing concept of a primary light source originating from a "primary column" about the path of the incident particle, plus a contribution from those energetic secondary electrons which escape the primary column. This is demonstrated schematically in Fig. 2. The scintillation efficiency in the primary column is taken to be a function of *only* dE/dx of the incident particle. It is assumed for present purposes that the primary column has a sharply defined radius; this radius is expected to be a function of dE/dx, though the dependence may be weak. The analysis can be given without any further consideration of the nature of the primary column or the physical mechanism responsible for its existence.

We turn now to the mechanics of analyzing the experimental data of Fig. 1 according to the preceding discussion. The differential light output per unit path length of the primary is given by

$$\left(\frac{dL}{dx}\right)_t=\left(\frac{dL}{dx}\right)_p+\left(\frac{dL}{dx}\right)_\delta=\left(\frac{dL}{dE}\right)_p\left(\frac{dE}{dx}\right)_p+\left(\frac{dL}{dE}\right)_\delta\left(\frac{dE}{dx}\right)_\delta. \quad (1)$$

Dividing by

$$(dE/dx)_t=(dE/dx)_p+(dE/dx)_\delta, \quad (2)$$

we obtain

$$(dL/dE)_t=(1-F)(dL/dE)_p+F(dL/dE)_\delta, \quad (3)$$

where F is defined as

$$F\equiv\frac{(dE/dx)_\delta}{(dE/dx)_t}$$

and represents the fractional energy loss of the primary which is deposited *outside* the primary column. In the above equations the subscripts t, p, and δ refer to total, primary, and delta ray. The scintillation efficiency $(dL/dE)_p$ refers to the efficiency in the primary column and is a function only of $(dE/dx)_p$. It is in fact $(dL/dE)_p$ which is the subject of the previous treatment of the saturation process.[1] The scintillation efficiency $(dL/dE)_\delta$ applies to electrons in the region below 22 keV, as 22 keV is the maximum delta-ray energy encountered in the experiments of Fig. 1. The minimum energy delta ray of interest is about 1 keV, determined by the radius of the primary column. In the range 1–22 keV, $(dL/dE)_\delta$ is very nearly constant[1,4] equal to unity with the

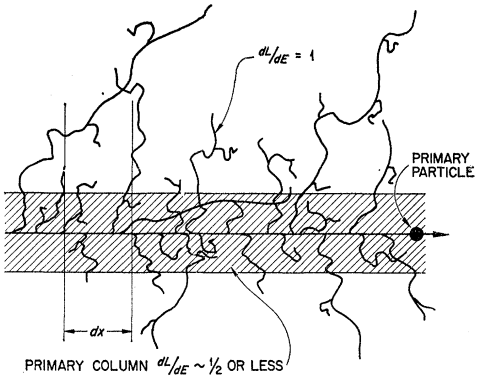

FIG. 2. Schematic diagram showing primary column and escaping delta rays.

[4] C. D. Zerby, A. Meyer, and R. B. Murray, Nuclear Instr. and Methods 12, 115 (1961).

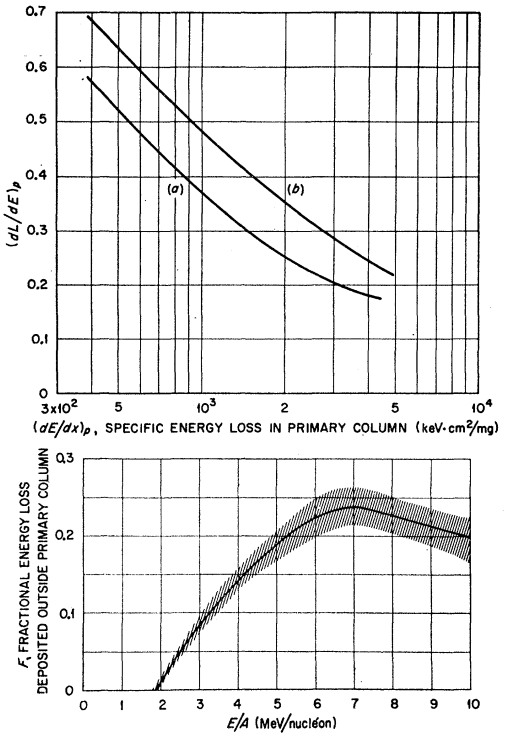

FIG. 3. Top: Curve (a) is the derived $(dL/dE)_p$ resulting from analysis of experimental data of Fig. 1 by a three-step iteration. For comparison, curve (b) was previously calculated on the basis of the saturation mechanism and is reproduced from reference 1. Bottom: Derived curve of F as a function of E/A (MeV per nucleon) from a three-step iteration. F is the fractional energy deposited outside of the primary column. The curve shown is a numerical average of the curves for the six particles B^{10}, C^{12}, N^{14}, O^{16}, F^{19}, Ne^{20}. Individual curves for all six particles fall within the shaded area.

normalization adopted in Fig. 1. We therefore take $(dL/dE)_\delta = 1.0$, and Eq. (3) becomes

$$(dL/dE)_t = (1-F)(dL/dE)_p + F. \tag{4}$$

Consideration of the expressions for $(dE/dx)_\delta$ and $(dE/dx)_t$ (see next section and reference 5) indicates that the ratio F should be a function only of the primary column radius and the energy per nucleon E/A of the incident particle. If the primary column radius is only weakly dependent on $(dE/dx)_p$ then F is determined principally by E/A. Thus, it should be possible to find a single curve for $(dL/dE)_p$ vs $(dE/dx)_p$ and a (nearly) universal curve for F as a function of E/A, starting from the experimental values of $(dL/dE)_t$ vs $(dE/dx)_t$ in Fig. 1. The procedure required to find such functions is an iterative one based on Eq. (4) plus the relation

$$\left(\frac{dE}{dx}\right)_t = \frac{(dE/dx)_p}{(1-F)}, \tag{5}$$

which follows directly from Eq. (2) and the definition of F. It is also necessary to know the relation between $(dE/dx)_t$ and E/A for each particle. This is taken from the curves of Newman and Steigert,[2] their Fig. 3. The end point of the iterative process is achieved if it is possible to find functions from Eqs. (4) and (5) meeting the above requirements. In practice, it is found that the iterations converge rather rapidly, and the result of a three-step iteration is given in Fig. 3. Curve (a) in the upper part of Fig. 3 is the final estimate of $(dL/dE)_p$ vs $(dE/dx)_p$. The lower half of Fig. 3 illustrates the derived results of F as a function of E/A. The shaded area contains six different curves for the six particles B^{10} through Ne^{20}. (No distinction is made between B^{10} and B^{11}.) The individual curves are not shown, in order to avoid confusion in the figure. It is noted that no systematic trend is observed in the displacement of the individual curves; the curves cross one another in a random fashion. This random crossing is attributed simply to the fact that the data of Fig. 1 are taken from experiment and are subject to a finite uncertainty. The curves of Fig. 1 are, in fact, the derivatives of measured pulse height versus energy relations, and are thus subject to the errors of establishing the slope of a curve. The smooth curve in the lower half of Fig. 3 is a numerical average of the individual curves for the six particles. It may be noted from Fig. 3 and Eq. (4) that the delta ray contribution to $(dL/dE)_t$ is a large effect. At large E/A, delta rays account for about half of the total emitted light.

Finally, curve (a) of Fig. 3 may be compared with the calculated dL/dE curve based on the previous saturation mechanism, see Fig. 6 of reference 1. This previously calculated curve is reproduced as curve (b) in the upper part of Fig. 3. It is seen that these curves are very similar in shape and differ only in their positions on the abscissa. The only meaningful comparison which can be made between these two curves is a comparison of their shapes, as the position of curve (b) with respect to dE/dx was not directly determinable from calculations, but was established by comparison with the general trend of experimental data.

ESTIMATED VALUES OF F

Having obtained F, the fractional energy deposited outside the primary column, as a function of E/A from the foregoing interpretation of experimental results, it is now appropriate to ask whether one can estimate F by other means which are independent of the above experiments. An accurate calculation of F from first principles is an exceedingly difficult, if not impossible, task. We have, however, undertaken several *approximate* calculations which should provide information on upper and lower bounds for F. The starting point in any calculation of F is a knowledge of the radius of the primary column. This radius is not known *a priori* and must be considered as a parameter to be determined

[5] H. A. Bethe and J. Ashkin, *Experimental Nuclear Physics*, edited by E. Segrè (John Wiley & Sons, Inc., New York, 1953), Vol. I, Part II.

on the basis of fitting calculated values of F to the curves in Fig. 3 determined from experiment. If the saturation mechanism is responsible for the primary column, then the column radius for heavy ions is expected to be of order hundreds of Angstroms and a slowly varying function of dE/dx. We will find, in fact, that the experimentally derived curves are bracketed by calculated upper and lower bounds for F if the column radius is taken to be about 400 Å.

We turn now to the details of estimating F. The total stopping power $(dE/dx)_t$ which enters into the denominator of F is taken directly from the curves of Newman and Steigert[2] as indicated in the preceding section. The burden of estimating F thus lies with the numerator $(dE/dx)_\delta$. In attempting to estimate the numerator, the first consideration must be the question of the number and energy distribution of secondary electrons in the 1–22 keV region. For electrons which are loosely bound to ions of the stopping medium, the secondary electron spectrum is given by the Rutherford distribution. On this basis the number of delta rays emitted in the energy interval ϵ_0 to $\epsilon_0+d\epsilon_0$, per cm path length of the primary particle, is given by

$$\frac{dn}{dx}=\frac{2\pi e^4 z^{*2}\rho_{\text{eff}}}{mV^2}\frac{d\epsilon_0}{\epsilon_0{}^2}, \tag{6}$$

where z^* and V are the effective charge and velocity of the incident particle, e and m are the electronic charge and mass, and ρ_{eff} is the density of loosely bound electrons in the stopping medium such that the Rutherford distribution is applicable. In considering the binding energies of various electrons in NaI, it is clear that Eq. (6) cannot be applied to the K- and L-shell electrons of iodine, for which the binding energies are 33 keV and about 5 keV. The contribution of these electrons to the delta-ray spectrum can be estimated,[6] however, and it is found for the projectiles of interest here that the total cross section for ionizing the iodine K or L shell is completely negligible in comparison with the Rutherford cross section. The binding energies of N- and O-shell electrons in iodine, and L-shell electrons in sodium, are all much smaller than the delta ray energies of present interest, so that these electrons should be well described by Eq. (6). The M-shell electrons of iodine and K-shell electrons of sodium represent intermediate cases, in which the binding energies are about 1 keV or less. In the present calculation the lowest energy delta ray which contributes to $(dE/dx)_\delta$ is about 1 keV for all E/A while the principal contribution arises from delta rays of considerably higher energy for E/A of 2 or 3 MeV/nucleon and greater. We have accordingly included the iodine M-shell electrons and sodium K-shell electrons in Eq. (6). In so doing, dn/dx is subject to the greatest uncertainty at low values of E/A and should be best at large E/A. The final result of these considerations is that ρ_{eff} includes 54 of the possible 64 electrons in NaI, neglecting the K- and L-shell electrons of iodine.

The effective charge z^* of the primary particle is a function of its velocity, and is taken from Roll and Steigert,[7] their Fig. 10. The charge z^* differs significantly from the full nuclear charge z only at low E/A.

If we express distance in mg/cm² and energy in keV, then (6) becomes

$$\frac{dn}{dx}=\frac{2.57\times10^4}{(E/A)}z^{*2}\frac{d\epsilon_0}{\epsilon_0{}^2}. \tag{7}$$

The problem is now to compute the energy deposited outside the primary column starting from a source described by Eq. (7). This calculation is approached in three different approximations described below.

A. Isotropic Emission

In this approximation, it is assumed that a delta ray is isotropically scattered in the crystal reference frame immediately after creation. The delta ray then suffers multiple scattering until it finally comes to rest at distance r from its origin. All delta rays of energy ϵ_0 will be contained within a sphere whose radius corresponds to their range. The concept of electron range may have several meanings; in particular it is possible to distinguish experimentally between the *maximum* range and the *practical* range. In the present section the practical range is more appropriate as we wish to describe the distribution of the majority of the electrons. The small fraction of the distribution whose range exceeds the practical and extends to the maximum is of little consequence. In the energy interval of interest here it is found experimentally that the practical range-energy relation can be reasonably well described in various stopping media by a function of the form $R_p=a\epsilon_0{}^n$, where both a and n are constants.[8,9] With R_p in mg/cm² and ϵ_0 in keV, and considering NaI as intermediate between aluminum and gold, we find $a=0.012$ and $n=1.35$. By virtue of multiple scattering, only a very small fraction of electrons penetrate a distance comparable with the range R_p. There will thus be a distribution of stopped electrons over the entire sphere from the origin to R_p, and this distribution can be represented by a density function $D(r,R_p)$. This density function is, of course, not known, and in fact may even have a different shape for different energy electrons. For very low energy electrons where a diffusion treatment is valid, the density function is of the form e^{-r^2}. The approach taken in the present work is to adopt the simplest possible form for the

[6] E. Merzbacher and H. W. Lewis, *Encyclopedia of Physics*, edited by S. Flügge (Springer-Verlag, Berlin, 1958), Vol. 34, p. 166.

[7] P. G. Roll and F. E. Steigert, Nuclear Phys. **17**, 54 (1960).

[8] H. Kanter, Phys. Rev. **121**, 461 (1961).

[9] H. Kanter and E. J. Sternglass, Phys. Rev. **126**, 620 (1962).

density function, consistent with the requirement that it be zero at the range R_p and reach a maximum at some smaller value of r. Thus, for unit source strength under isotropic emission we take

$$D(r,R_p)=(3/\pi R_p^3)(1-r/R_p), \tag{8}$$

where the factor $3/\pi R_p^3$ is required for normalization. Fortunately, the results to be derived from the present analysis are rather insensitive to the shape of the density function, as will be indicated later. The assumption of Eq. (8), therefore, does not seriously limit the conclusions to be drawn. From (8), it follows that the probability that an electron whose initial energy is in the interval ϵ_0 to $\epsilon_0+d\epsilon_0$ will stop at a radial distance between r and $r+dr$ is simply

$$(12/R_p^3)(1-r/R_p)r^2dr.$$

We must now trace an electron of initial energy ϵ_0 from its point of origin, along a winding path, to its point of capture a distance r from the source, and ask for the energy of the electron at the radial distance ρ. This is treated by considering that the actual, winding path is stretched out to the range R_p, and we now ask for the electron's energy at a radial distance $(R_p/r)\rho$. Application of the foregoing range-energy relation yields the result

$$\epsilon(\rho)=(1-\rho/r)^{1/n}\epsilon_0. \tag{9}$$

The final task is to combine the above prescriptions with the appropriate geometry. Consider an electron of initial energy ϵ_0 which is born along the axis of the primary column, whose radius is r_c, and which travels a radial distance between r and $r+dr$. The energy deposited outside the primary column by such an electron is

$$\frac{12\epsilon_0}{R_p^3}\left(1-\frac{r}{R_p}\right)r^2dr\int_{\arcsin(r_c/r)}^{\pi/2}\left(1-\frac{r_c}{r\sin\theta}\right)^{1/n}\sin\theta d\theta$$

where θ is the polar angle of radius vector r measured from the column axis. The *total* energy deposited outside the column by one electron of initial energy ϵ_0 is obtained by integrating the above expression over all possible values of r, viz., from r_c to R_p. The final expression now requires only the source term, Eq. (7), and a final integration over all appropriate values of ϵ_0:

$$\left(\frac{dE}{dx}\right)_\delta\left(\frac{\text{keV}-\text{cm}^2}{\text{mg}}\right)=\frac{3.08\times10^5}{(E/A)}z^{*2}\int_{\epsilon_0^{\min}}^{\epsilon_0^{\max}}\frac{d\epsilon_0}{R_p^3\epsilon_0}\times\int_{r_c}^{R_p}\left(1-\frac{r}{R_p}\right)r^2dr\int_{\arcsin(r_c/r)}^{\pi/2}\left(1-\frac{r_c}{r\sin\theta}\right)^{1/n}\times\sin\theta d\theta \tag{10}$$

where $\epsilon_0^{\min}=(r_c/a)^{1/n}$ and $\epsilon_0^{\max}=(4/1822)(E/A)$. This expression for $(dE/dx)_\delta$ is based on the assumption of isotropic emission; it completely neglects the initial forward motion of delta rays which has the effect of containing the delta-ray track (especially one of high energy) within the primary column. This assumption is therefore an unrealistic limiting case, and Eq. (10) should give an *overestimate.*

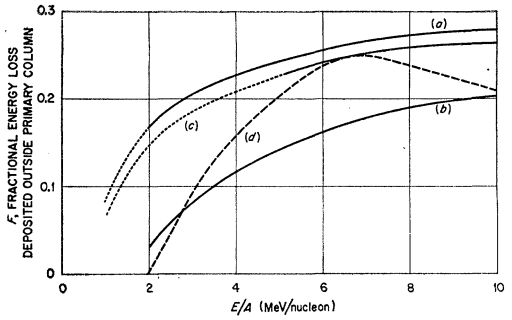

FIG. 4. Curve (a): calculated "point isotropic" source. Curve (b): calculated "point anisotropic" source. Curve (c): calculated on basis of Spencer's energy deposition function. Curve (d): derived from experiment on basis of Eq. (4) and iterative procedure. All curves apply to O^{16} in NaI(Tl). Dotted curves indicate regions of greatest uncertainty.

The integrals of Eq. (10) have been evaluated numerically with a digital computer for the various charged particles and for several values of r_c. The result for O^{16} with $r_c=400$ Å (independent of dE/dx) is shown as curve (a) of Fig. 4. It is seen to lie above the experimentally derived curve for O^{16}, shown as curve (d). At this point it should be re-emphasized that the choice of $r_c=400$ Å is made *a posteriori* in such a way that the above overestimate and the underestimate described in (B) below bracket the experimental result.

The calculated curve for only one projectile, O^{16}, is shown in Fig. 4 in order to avoid confusion. Calculated curves for the other particles are very closely superposed on the O^{16} curve, and are in fact almost indistinguishable on the scale of this figure.

B. Extreme Anisotropic Emission

In this approximation it is assumed that the displacement vector from point of origin of the delta ray to its stopping point has the same direction as the original direction of motion when the delta ray is created. The delta ray is, of course, subject to multiple scattering, and the actual path is a winding one. The present approximation is equivalent to assuming that the electron's path is curled about the displacement vector. The purpose of this approximation is to treat the geometry in the opposite extreme to Sec. A above. Under the present assumption a high-energy delta ray, which is necessarily emitted at a small angle with the cylinder axis, will lose much or all of its energy in the primary column. The calculated $(dE/dx)_\delta$ under this circumstance should represent a lower limit.

The calculation is similar to that of Sec. A above, but with a slightly more complicated geometry. The

source function is, of course, the same as given by Eq. (7). For comparison with the isotropic case we must take the density distribution function to be of the same form, viz. $(1-r/R_p)$. It must be carefully noted, however, that electrons in the energy interval ϵ_0 to $\epsilon_0+d\epsilon_0$ are all emitted into a conical shell defined by θ to $\theta+d\theta$, since the initial energy ϵ_0 is directly related to θ by

$$\epsilon_0=2mV^2\cos^2\theta=(4/1822)(E/A)\cos^2\theta. \quad (11)$$

A brief consideration of the geometry reveals that for an electron whose initial energy is in the interval ϵ_0 to $\epsilon_0+d\epsilon_0$, the probability of stopping at a distance r from the origin is $(12/R_p^3)(1-r/R_p)r^2dr$. This is identically the same as the probability in the isotropic case, as it must be.

We now consider an electron whose initial energy is in the interval ϵ_0 to $\epsilon_0+d\epsilon_0$. The energy which it deposits outside the cylinder is

$$\frac{12\epsilon_0}{R_p^3}\int_{r_c/\sin\theta}^{R_p}\left(1-\frac{r}{R_p}\right)\left(1-\frac{r_c}{r\sin\theta}\right)^{1/n}r^2dr. \quad (12)$$

From Eq. (11), $\sin\theta=(1-w\epsilon_0)^{\frac{1}{2}}$, where

$$w=[(4/1822)(E/A)]^{-1}.$$

The final expression now requires the source term and an integration over all contributing ϵ_0:

$$\left(\frac{dE}{dx}\right)_\delta\left(\frac{\text{keV}-\text{cm}^2}{\text{mg}}\right)=\frac{3.08\times10^5}{(E/A)}z^{*2}\int_{\epsilon_0{}^L}^{\epsilon_0{}^U}\frac{d\epsilon_0}{R_p{}^3\epsilon_0}$$

$$\times\int_{r_c(1-w\epsilon_0)^{-1/2}}^{R_p}\left(1-\frac{r}{R_p}\right)\left(1-\frac{r_c}{r(1-w\epsilon_0)^{\frac{1}{2}}}\right)^{1/n}r^2dr. \quad (13)$$

In (13), $\epsilon_0{}^L$ and $\epsilon_0{}^U$ are the lower and upper values of the energy for which it is energetically possible for an electron to escape the cylinder. These limits are found as the lower and upper roots to the equation

$$a^2\epsilon_0{}^{2n}(1-w\epsilon_0)-r_c{}^2=0.$$

The integrals of Eq. (13) have been evaluated numerically with a digital computer for the various charged particles and for several values of r_c. The result for O^{16} with $r_c=400$ Å (independent of dE/dx) is shown as curve (b) of Fig. (4). This approximation is expected to be a lower limit, and it is seen to lie below the experimentally derived curve for O^{16}, shown as curve (d).

C. Energy Dissipation Function

This calculation departs from the approach used in Secs. A and B above, and attempts to calculate $(dE/dx)_\delta$ from a substantially different point of view. In this section, we carry over only the source function, Eq. (7). The present calculation employs the electron energy dissipation functions of Spencer,[10] in particular Spencer's function for a point isotropic source of 25-keV electrons in copper. Spencer's function $J(x)$ is given as a function of the reduced coordinate $x=r/R_m$, and $J(x)$ is defined as

$$J(x)=\frac{I(r)}{(d\epsilon/dr)_{\epsilon_0}}, \quad (14)$$

where $I(r)dr$ is the (average) energy per electron dissipated in the spherical shell between r and $r+dr$. In the Spencer formulation the range R_m corresponds to the *maximum* electron range, i.e., the total distance traveled along the winding path. It is this range which is given by the stopping-power theory of Bethe[5] and which has been calculated by Nelms.[11] This theoretical range should also correspond to the experimental maximum range. In the present case, R_m is needed as a function of ϵ_0 down to about 1 keV. This was calculated according to the Bethe stopping-power theory, although such a calculation is subject to question at such low energies. It is noted, however, that the calculated values agree reasonably well with the experimental maximum range,[9] considering NaI as intermediate between aluminum and gold.

The use of the energy dissipation function in the present problem involves several approximations, the first being the extrapolation of this function for 25-keV electrons (the lowest energy considered by Spencer) into the energy region of interest here which extends from 22 keV down. The rationale is that the shape of $J(x)$ is not particularly sensitive to energy from 100 to 25 keV, and it is assumed that this shape is reasonably the same at least for the high-energy delta rays encountered here. This treatment is, therefore, best at large E/A, and is most uncertain at low E/A. Again, the detailed shape of this curve need not be well known as the calculation proves to be quite insensitive to the details of the distribution function. The second assumption involves the extrapolation from calculated curves in copper to the present medium, NaI. Copper was chosen as its Z which is intermediate between Z of Na and I. A further approximation is the assumption of isotropic emission of delta rays. This approximation, as in Sec. A, should lead to an overestimate of $(dE/dx)_\delta$.

The use of the energy dissipation function proceeds as follows. For an electron of energy ϵ_0, the energy deposited in a spherical shell of radius r is $I(r)dr$. The fraction of this spherical shell which lies outside a cylinder of radius r_c is $[1-(r_c/r)^2]^{\frac{1}{2}}$, so that the energy deposited outside the cylinder is $I(r)dr[1-(r_c/r)^2]^{\frac{1}{2}}$. The total energy deposited outside the cylinder by

[10] L. V. Spencer, *National Bureau of Standards Monograph* I, *September, 1959* (Superintendent of Documents, U. S. Government Printing Office, Washington 25, D. C.).

[11] Ann T. Nelms, *National Bureau of Standards Circular No. 577 Supplement, 1958* (Superintendent of Documents, U. S. Government Printing Office, Washington 25, D. C.).

one electron is therefore

$$\int_{r_c}^{R_m} I(r)\left[1-\left(\frac{r_c}{r}\right)^2\right]^{\frac{1}{2}} dr = R_m\left(\frac{d\epsilon}{dr}\right)_{\epsilon_0}\int_{r_c/R_m}^{1} J(x)\left[1-\left(\frac{r_c}{xR_m}\right)^2\right]^{\frac{1}{2}} dx. \quad (15)$$

Introducing the source function (7) and integrating over all contributing energies, we obtain

$$\left(\frac{dE}{dx}\right)_\delta\left(\frac{\text{keV}-\text{cm}^2}{\text{mg}}\right) = \frac{2.57\times10^4}{(E/A)}z^{*2}\int_{\epsilon_0^{\min}}^{\epsilon_0^{\max}} R_m\left(\frac{d\epsilon}{dr}\right)_{\epsilon_0}\frac{d\epsilon_0}{\epsilon_0^2} \times\int_{r_c/R_m}^{1} J(x)\left[1-\left(\frac{r_c}{xR_m}\right)^2\right]^{\frac{1}{2}} dx. \quad (16)$$

In connection with Eq. (16) it should be kept in mind that $J(x)$ is taken from 25-keV electrons and is applied to the entire spectrum of delta rays. We note from (14) and the definitions that

$$\int_0^1 J(x)dx=\frac{\epsilon_0}{R_m(d\epsilon/dr)_{\epsilon_0}},$$

and this quantity is a constant whose numerical value is 1.70. It must therefore remain a constant over the entire delta-ray spectrum and may be taken out of the energy integral of (16). Consideration of the calculated (and experimental) values for R_m and $(d\epsilon/dr)_{\epsilon_0}$ indicates that this requirement leads to an overestimate of $(dE/dx)_\delta$. Thus Eq. (16) is expected, for two reasons, to give an upper limit to F.

The integrals of Eq. (16) were numerically evaluated on a computer and the result for O^{16} with $r_c=400$ Å (independent of dE/dx) is shown as curve (c) of Fig. (4). This curve is seen to lie above the experimentally derived curve (d). Curve (c) is considered to be in question at small E/A by virtue of the approximations discussed above, and is shown dashed in this region.

DISCUSSION

The three calculations presented above are based on various assumptions which surely cannot be justified rigorously. It is therefore important to examine the sensitivity of the result to changes in the assumptions. Perhaps the weakest point of Secs. A and B is the assumption of a density distribution function of the form $(1-r/R_p)$. As a check on the influence of this distribution function, a second function was chosen of the form $[r/R_p(1-r/R_p)]^2$. This function is bell-shaped reaching a maximum at $R_p/2$, and has the effect of pushing the electron distribution out to larger r. The calculations of Secs. A and B were repeated with this function, and were found to be very nearly the same as with the original distribution. For example, with the new distribution function, the value of F at $E/A=10$ was increased by about 0.007 for both the isotropic and anisotropic cases. At $E/A=3$, F was increased by about 0.01.

The effect of a different range-energy relation was examined by changing the exponent n from 1.35 to 1.65, which is artificially large. In the point isotropic case the effect of a greater exponent is to increase F by a roughly constant amount of 0.02. Thus, an unrealistically large range does not significantly alter the conclusions.

The calculations presented here are therefore relatively insensitive to the details of how the electron energy deposition is treated. This redeeming feature arises from the fact that we are dealing primarily with electrons whose range is many times greater than the column radius. The range of a 4-keV electron is five times the column radius and the range of a 20-keV electron is 45 times the column radius, assuming a radius of 400 Å. Clearly, the present calculational methods are most in question at low E/A, where the delta-ray range becomes comparable with the column radius.

Changes in the column radius, of course, shift the calculated curves and alter the shape somewhat at low E/A. The assumption of a column radius of 500 Å lowers the point isotropic curve (a) of Fig. 4 at $E/A=10$, from 0.28 to 0.26.

It is concluded that the calculated upper and lower bounds bracket the experimentally derived F curve for a column radius of 400 Å, with an uncertainty of order 100 Å or greater.

Finally, it may be noted that changing the distribution function, changing the exponent in the range-energy relation, and changing the primary column radius affects the fractional energy deposited outside the column by a practically constant shift for all values of E/A. Thus, the shapes of the calculated curves are practically unchanged by all these operations. A detailed comparison with the shape of the experimental F curve is clearly hazardous, especially in view of the uncertainties inherent in this curve. (Uncertainties in the pulse height vs energy measurement[2] amount to about 1% at high E/A and 2% at low E/A; uncertainties in the *slope* of this curve, dL/dE, are of course greater.) In spite of these uncertainties, several comments may be made regarding the experimental F curve. First, the fall-off above an E/A of about 7 occurs because the experimental dL/dE is apparently constant in this region. If dL/dE were not strictly constant, but slowly increased with energy, the effect would be to raise the experimental F curve at the highest E/A. In this regard it should be noted that a technical effect exists which tends to reduce the meas-

ured pulse height at high energy (relative to that at low energy) and hence render the observed dL/dE too small at high energies. This effect is associated with the pulse decay time; the effective decay time becomes slower with decreasing dE/dx (increasing energy)[12] so that, with a fixed clipping time, one measures a smaller fraction of the total light at higher energies. Correction for this effect would raise the experimental F curve at the high energy end.

Second, it may be noted that the experimental F curve below an E/A of about 5 is steeper than any calculated curve. Several effects may enter into the shapes of the calculated curves: (1) At high values of E/A, the iodine L-shell electrons may begin to contribute to the delta-ray effect; (2) at low values of E/A, the contribution from iodine M-shell electrons may be reduced below the Rutherford cross section; and (3) if the primary column radius becomes greater with increasing dE/dx, then F will be reduced in the low energy region. Each of these three effects acts to steepen the calculated curves, and is therefore in a direction to improve agreement with the experimental curve at low E/A.

SUMMARY

It is concluded that the interpretation of heavy ion data presented here is internally consistent since it is possible to find, from experimental data, functions for $(dL/dE)_p$ and F which satisfy the required equations for the entire set of incident heavy ions. The experimentally derived curve of F is supported, as to its general shape and magnitude, by approximate calculations based on a column radius of about 400 Å, independent of dE/dx. The present analysis and the available experimental data are not sufficiently precise to determine whether the column radius is a function of dE/dx.

The analysis given here has been based entirely on data obtained with NaI(Tl), as these are apparently the most complete set of data available. The interpretation, however, is not restricted to NaI(Tl) but should be equally applicable to other inorganic scintillators.

The interpretation presented in this paper should be amenable to a direct experimental check. For a particle at low E/A all the emitted light is expected to be from the primary column and the pulse decay time should be characteristic of a high-dE/dx particle (fast decay time). At large values of E/A, about half the emitted light is attributed to delta rays, and the decay time from this contribution should be characteristic of electrons (slow decay time). Therefore, if one compares the pulse shapes from two different primary particles at the same dE/dx such that one particle is at low E/A and the other at high E/A, a distinct difference in effective decay time should be observed. As an example, C^{12} and O^{16} at 2000 keV-cm^2/mg fit this condition. The effect would probably be most pronounced in CsI(Tl) as this crystal shows the greatest dependence of pulse shape on stopping power. This experiment would be best performed with a thin crystal, such that the high-E/A particle would lose only a fraction of its energy and the pulse shape would be characteristic of a reasonably well-defined dE/dx. A crystal thickness of order 0.001 in. should be appropriate. The low-E/A particle can be completely stopped in the crystal as its pulse shape should be characteristic of the primary column over its entire path.

ACKNOWLEDGMENTS

The authors are indebted to Mrs. J. G. LaTorre of the Mathematics Panel of this laboratory, who performed all the numerical calculations. We wish to acknowledge very helpful discussions with R. D. Birkhoff. We also wish to thank F. E. Steigert of Yale University and H. Kanter of Westinghouse Research Laboratory for valuable discussions and for communicating results of their research. D. K. Holmes has kindly reviewed the manuscript.

[12] M. Bormann, G. Anderson-Lindström, H. Neuert, and H. Pollehn, Z. Naturforsch. **14a**, 681 (1959).